UPDATE

The Right Heart and Pulmonary Circulation (II)

Imaging Techniques and the Evaluation of the Right Heart and the Pulmonary Circulation

Javier Sanz,[a] Leticia Fernández-Friera,[a] and Sergio Moral[b]

[a]The Zena and Michael A. Wiener Cardiovascular Institute and Marie-Josee and Henry R. Kravis Center for Cardiovascular Health, Mount Sinai School of Medicine, New York, NY, USA
[b]Departamento de Cardiología, Hospital Universitario Dr. Josep Trueta, Girona, Spain

Since the right side of the heart and the pulmonary circulation are regarded as secondary components of the circulatory system, their role in disease has traditionally not received the same attention as their counterparts in the systemic circulation. This was partly because precise noninvasive study of these structures was difficult. For many years, chest radiography and invasive angiography were the only techniques available for imaging the minor circulation. The development of transthoracic echocardiography and nuclear techniques has produced a significant leap forward for noninvasive imaging, particularly of the right ventricle. More recently, novel echocardiographic techniques, and advances in computed tomography and magnetic resonance imaging, in particular, have expanded our diagnostic armamentarium and provided new insights into the anatomy and function of the pulmonary circulation in both health and disease. This article contains a review of the current status of techniques for imaging the right side of the heart and the pulmonary circulation.

Key words: *Right ventricle. Pulmonary circulation. Imaging*

Técnicas de imagen en la evaluación del corazón derecho y la circulación pulmonar

Considerados componentes secundarios del sistema circulatorio, los papeles del corazón derecho y la circulación pulmonar en la enfermedad no recibieron la misma atención que sus análogos sistémicos por mucho tiempo. Esto se debió en parte a la dificultad de estudiar estas estructuras con precisión y de forma no invasiva. Durante muchos años la radiografía de tórax y la angiografía invasiva fueron las únicas modalidades de imagen disponibles para evaluar la circulación menor. El desarrollo de la ecografía transtorácica y de técnicas nucleares constituyó un importante avance en imagen no invasiva, particularmente del ventrículo derecho. Más recientemente, nuevas técnicas ecocardiográficas, avances en tomografía computerizada y, particularmente, en resonancia magnética han aumentado nuestro armamentario diagnóstico y proporcionan un mayor entendimiento de la anatomía y función de la circulación derecha tanto en la salud como en la enfermedad. En este artículo revisaremos el estado actual de las técnicas de imagen en el corazón derecho y la circulación pulmonar.

Palabras clave: *Ventrículo derecho. Circulación pulmonar. Imagen.*

INTRODUCTION

The right heart chambers and pulmonary circulation have important roles in cardiovascular homeostasis both in normal and pathologic conditions. However, changes in their anatomy and function associated with disease have often been considered less relevant than those occurring on the left side, particularly in the clinical setting. One of the reasons for this disparity is the earlier and broader availability of noninvasive imaging modalities for accurate and reliable evaluation of left ventricular performance. For a long time, invasive right heart catheterization and contrast angiography have been the reference standards for the study of the anatomy of the right heart and pulmonary circulation, as well as the hemodynamic impact of different diseases. Over the past 3 decades there has been a progressive shift to a noninvasive approach, particularly because of improvements in echocardiography, computed

Correspondence: Dr J. Sanz.
Cardiovascular Institute, Mount Sinai Hospital,
One Gustave L Levy Place, Box 1030. New York, NY 10029.
E-mail: Javier.Sanz@mssm.edu

ABBREVIATIONS

CT: computed tomography
CTEPH: chronic thromboembolic pulmonary hypertension
DSA: digital subtraction angiography
MRI: magnetic resonance imaging
PA: pulmonary artery
PH: pulmonary hypertension
RV: right ventricle
TAPSE: tricuspid annular plane systolic excursion
TDI: tissue Doppler imaging
V/Q: ventilation/perfusion ratio
2D: two-dimensional
3D: three-dimensional

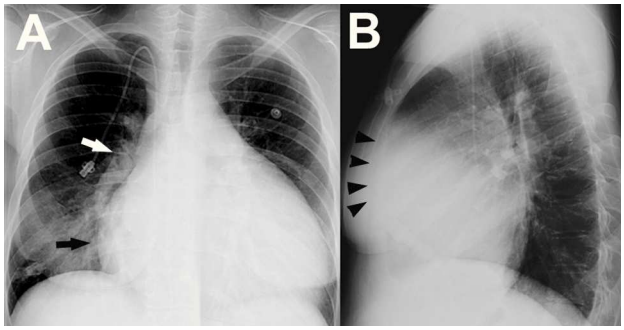

Figure 1. A: postero-anterior chest roentgenogram in a patient with idiopathic pulmonary hypertension showing marked cardiomegaly, right atrial enlargement (black arrow), dilated central pulmonary arteries (right pulmonary artery, white arrow) and diffuse reduction in peripheral vascularity. An intravascular catheter for the infusion of medication is also seen. B: lateral chest x-ray in the same patient demonstrating enlarged right ventricle (black arrowheads).

tomography (CT) and magnetic resonance imaging (MRI).

The optimal imaging modality should be able to evaluate not only the pulmonary circulation and the right cardiac chambers, but also the left chamber and, ideally, pulmonary ventilation. It would be desirable that it provides high resolution anatomical delineation together with functional information such as blood flow patterns or dynamic changes throughout the cardiac cycle. It should be accurate, reproducible, widely available, completely non-obtrusive and inexpensive. Unfortunately, no single modality fulfills all these requirements and each has specific strengths and limitations. In this review we will address specific applications of different imaging techniques for the study of the right heart and pulmonary circulation, with a particular emphasis on pulmonary hypertension (PH).

CHEST RADIOGRAPHY

A chest roentgenogram is cheap and widely available, but provides only rough information regarding cardiopulmonary status. Although fairly sensitive, abnormalities in the plain chest x-ray often lack specificity.[1] In the case of PH, radiographic signs tend to correlate poorly with disease severity and commonly occur late in its course. Right atrial enlargement is best noted as a prominently convex lower right heart border, as the posteroanterior projection (Figure 1A). Right ventricular (RV) dilatation is best detected on the lateral view when the cardiac silhouette occupies >40% of the lower retrosternal space (Figure 1B). In addition, enlargement of the right heart chambers leads to posterior rotation of the cardiac axis and lateral displacement of the RV outflow tract, which results in a more prominent "pulmonary artery" (PA) contour in the left cardiac border. A radiographic examination can potentially identify signs of underlying etiologies, such as lung parenchymal abnormalities or left heart disease.[2]

Regarding the pulmonary circulation, enlargement of the central pulmonary arteries can be quantified by adding the horizontal distances of the first divisions of the right and left pulmonary arteries to the midline, divided by the maximum transverse diameter of the thorax. A ratio >0.38 is often indicative of elevated pulmonary pressures.[3] Diameters of the right and left descending PA diameters above 16 and 18 mm, respectively, on posteroanterior projections also indicate PH.[4] Whereas peripheral vessel density increases in systemic-to-pulmonary shunts ("shunt vascularity"), a typical finding of advanced PH is reduced peripheral vessel caliber and density ("pruning").[2,5] Post-stenotic dilatation of the main and left PA can be present in cases of pulmonary valve stenosis, whereas dilated PA and RV without shunt vascularity or pruning may indicate pulmonary regurgitation. In addition, signs of PH with normal lung parenchyma coupled with regional oligemia are suggestive of chronic thromboembolic PH (CTEPH).[2]

ECHOCARDIOGRAPHY

Echocardiography is the most commonly used imaging modality for routine clinical evaluation of the RV since it is widely available, extremely safe and relatively inexpensive.[5] The combination of 2-dimensional (2D), M-mode, and Doppler echocardiography allows for the simultaneous

assessment of ventricular and valvular function. It provides invaluable hemodynamic information with flow characterization of both the left and right heart. However, it is not well suited for studying the pulmonary vasculature (except for the main PA). In addition, standard techniques are limited due to the complex RV geometry, retrosternal position, and the marked load dependence of RV function indices, so quantification is often only an estimation. Recent advances may be used for complementary information beyond standard 2D measurements (Table 1).

TABLE 1. **Echocardiographic Methods for the Assessment of the Right Ventricle and Pulmonary Circulation**

M-mode echocardiography
TAPSE
RV outflow tract fractional shortening
2D echocardiography
Linear dimensions to assess septum thickness and RV dimensions
Ventricular eccentricity index
Fractional area change
3D echocardiography
RV volumes
RV ejection fraction
Conventional Doppler echocardiography
Myocardial performance index
Dp/dt
Systolic, diastolic, and mean pulmonary artery pressures
Pulmonary vascular resistance
Pulmonary artery acceleration time
Tissue Doppler imaging
Spectral TDI
Color TDI
Strain imaging
One-dimensional strain rate
Two dimensional strain rate or speckle tracking
Intracardiac echocardiography

Dp/dt indicates delta pressure/delta time; RV, right ventricle; TAPSE, tricuspid annular plane systolic excursion; TDI, tissue Doppler imaging.

Standard Echocardiographic Modalities

Evaluation of the RV

Accurate evaluation of RV size, volume and, contractility requires a complete set of 2D standardized images.[6] Typical changes in RV volume and/or pressure overload include right atrial and RV enlargement, with or without RV hypertrophy, and RV systolic dysfunction (Figure 2A). A value of end-diastolic free RV wall thickness above 5 mm (measured in the subcostal 4-chamber view) indicates hypertrophy and is strongly associated with chronically increased afterload.[7]

RV volumes are difficult to quantify because of the complex RV geometry and the difficulty of tracing the markedly trabeculated endocardial surface. Hence, 2D methods that rely on Simpson's formula suffer from lack of standardization and tendency to underestimate volumes. Instead, visual estimation of the RV size relative to the left ventricle or measurements of transverse and longitudinal diameters are usually performed. An abnormal pattern of interventricular septal motion (leftwards displacement in systole or diastole when pressure or volume overload, respectively, are present) reflects RV hemodynamics. Left septal bowing leads to ventricular under-filling and reduced stroke volume, even in the presence of normal systolic function (Figure 2A). The left ventricular eccentricity index is calculated as the ratio of the antero-posterior to the septal-lateral short axis cavity dimension of the left ventricle. A value of 1 is considered normal,[8] and an elevated diastolic eccentricity index has been associated with death or pulmonary transplant in idiopathic PH.[9] In addition, the degree of septal curvature and its relation to the left ventricular free wall curvature can be used to estimate transeptal pressure gradients and RV systolic pressures.[10]

Longitudinal displacement of the RV annular segment toward the apex (tricuspid annular peak systolic excursion [TAPSE]) is measured with M-mode in the apical 4-chamber view. A value of <1.8 cm indicates RV dysfunction and has been shown to predict survival in PH.[11] This method shows a strong correlation with radionuclide angiography RV ejection fracion[12] even though it correlated poorly with MRI.[13] Although fast and simple, it is a one-dimensional approach, reflecting mostly regional (basal) RV systolic function. Assessment of RV outflow tract fractional shortening may add value to TAPSE. Right ventricular fractional area shortening is defined as the percentage of change in the RV chamber area in an apical 4-chamber view during the cardiac cycle, and seems to correlate best with MRI.[13] The Tei index or RV myocardial performance index is a global assessment of both RV systolic and diastolic function. It is the ratio of the total RV isovolumetric time (isovolumetric contraction plus relaxation intervals) divided by the RV ejection time.[14] The normal value is 0.28 (0.04), and an elevated index (≥0.83) is associated with increased cardiac mortality and lung transplantation in PH patients.[15] The Tei index has shown significant correlation with RV ejection fraction by nuclear ventriculography and has been reported to be less affected by loading conditions or heart rate.[14,16]

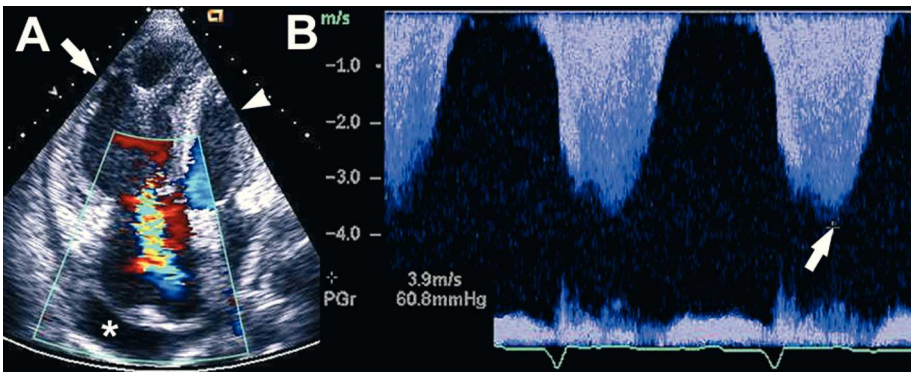

Figure 2. A: four-chamber view of a 2D echocardiogram in a patient with severe pulmonary hypertension demonstrating an enlarged right ventricle (white arrow), a small left ventricle (white arrowhead) and flattened septum. A pericardial effusion is indicated by the asterisk. In addition, color Doppler demonstrated the presence of tricuspid regurgitation. B: continuous Doppler recording of the tricuspid regurgitation jet allows measurement of a regurgitant peak velocity (white arrow) of 3.9 m/s or a calculated peak pressure gradient of 60.8 mm Hg between the right ventricle and the right atrium.

Hemodynamic Assessment of the Pulmonary Circulation

Doppler echocardiography allows non invasive estimation of PA pressures and vascular resistance. The tricuspid regurgitant jet is the most common method used in clinical practice to calculate the systolic PA pressure via the Bernoulli equation as $4v^2$ + right atrial pressure (Figure 2B), where v is the peak regurgitant velocity (m/s). Right atrial pressure is estimated from the inferior cava vein diameter and its respiratory changes. A diameter in long axis <1.5 cm with normal respiratory variation (~50%) corresponds to right atrial pressures <10 mm Hg.[6]

The peak velocity of the pulsed-Doppler envelope and the time to peak flow acceleration (acceleration time) in the main PA are reduced in PH. A shorter acceleration time (<100 ms) is suggestive of PH and a time <62 ms has been correlated with worsened survival in idiopathic PH.[17] However, the acceleration time is dependent on heart rate and cardiac output and has to be interpreted with caution. Diastolic PA pressure can be determined also from $4v^2$ + right atrial pressure, with v being in this case the velocity of the end-diastolic pulmonary regurgitant jet. Another contribution of Doppler echocardiography is the estimation of pulmonary vascular resistance, which is calculated as the ratio of tricuspid regurgitation velocity (m/s) to the velocity-time interval (cm) of the RV outflow. It has been validated in children with severe PH[18] and has shown excellent correlation with invasive measurements.[19] In addition, exercise echocardiography may reveal exercise-induced increments in systolic PA pressure, a finding that might represent early stages of pulmonary vascular disease.[20]

Emerging Echocardiographic Techniques

Three-Dimensional Echocardiography

In recent years, the introduction of new matrix transducers as well as advances in image acquisition and analysis have permited real-time 3D echocardiography in the clinical setting.[21] There are still limitations related to limited temporal resolution of real-time imaging or the need to average 4-7 cardiac cycles with full volume imaging, which may cause artifacts in cases of arrhythmia.

Direct visualization of the entire RV with 3D echocardiography is possible using the full volume mode acquisition. This capability is particularly attractive for the RV as it has the potential advantage to measure cardiac chambers without geometric assumptions. Both older[22] and more recent real-time 3D techniques[23,24] have been validated for RV volume quantification, information that can provide important prognostic information in various clinical scenarios such as congenital heart disease.[25] The non-planar geometry of the tricuspid valve has been demonstrated, as well as how RV contributes to functional tricuspid regurgitation.[26,27] Multiplane reconstruction analysis allows accurate evaluation of segmental RV geometry and function (Figure 3). In chronic PH secondary to left-sided heart disease, RV dilatation has been reported to occur mainly in segments closest to the outflow tract (basal and mid levels).[28]

Tissue Doppler Imaging (TDI)

Pulsed-wave Doppler at the tricuspid annulus can be used to measure low-frequency systolic and diastolic velocities that reflect longitudinal RV myocardial motion. Spectral TDI quantifies peak

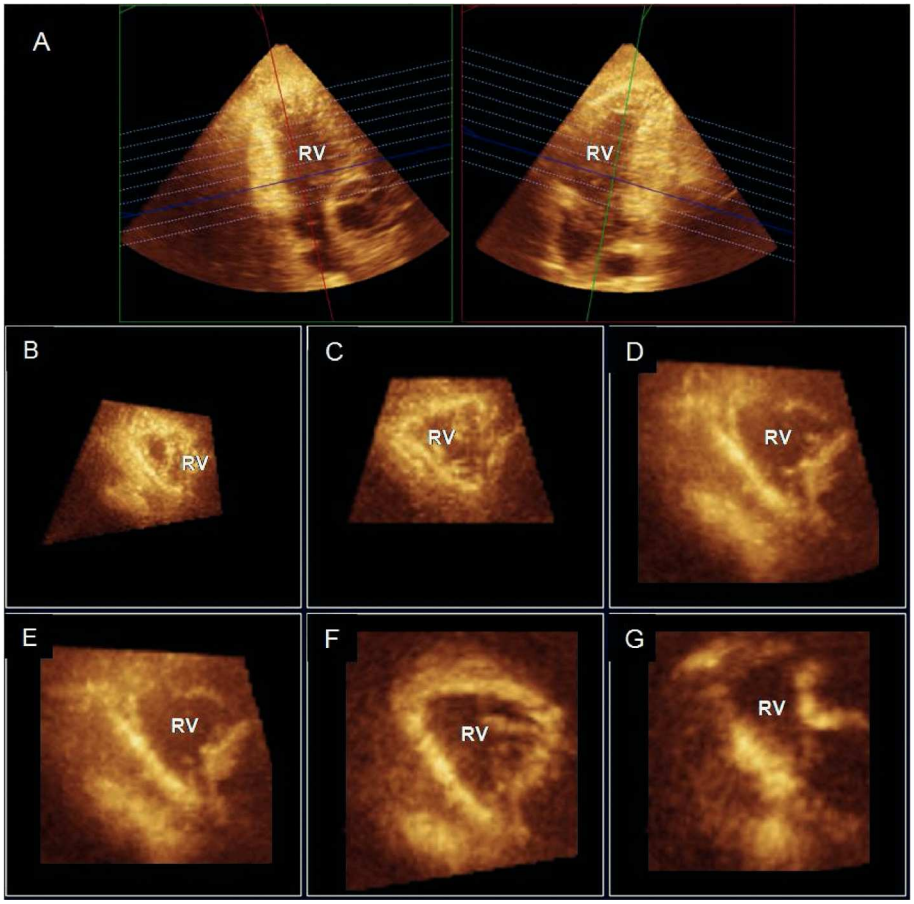

Figure 3. Real-time 3D echocardiogram (Full volume mode acquisition) of the right ventricle (RV) reformatted into coronal (A, right), sagittal (A, left), and multiple short-axis views showing segmental geometry of the RV (B, C: apex; D, E: mid; and F, G: basal segments).

velocities (Figure 4A). There are good correlations between TDI of the tricuspid annulus and RV ejection fraction quantified by radionuclide angiography.[29] A value of S' below 9.7 cm/s suggests abnormal RV contractility,[30] and may be useful in the detection of early RV dysfunction.[31] S' is also lower in patients with idiopathic PH than in normal controls, and is inversely related to PA pressures and resistance.[32] Myocardial acceleration during isovolumetric contraction is a new parameter of global RV systolic function, calculated as the maximal isovolumetric myocardial velocity divided by time to peak velocity. It appears to be less load dependent than other methods.[33] Regarding RV diastolic function, TDI may be a useful modality, combined with pulsed wave Doppler analysis of the tricuspid inflow, allowing the quantification of the E/A, E/E' and E'/A' ratios. Isovolumetric relaxation time can be considered a simple method to estimate systolic PA pressure when corrected for heart rate, and has been shown to increase progressively in the presence of PH.[34] However, results should be interpreted with caution when RV function is impaired.[35]

Color TDI acquires color-coded images of the RV and represents the average velocities within a specific region of interest (Figure 4B). It allows simultaneous evaluation of the annular, basal, mid, and apical segments within the same cardiac cycle in a reproducible fashion.[36] Besides quantification of myocardial velocity strain (percentage change in myocardial deformation) and strain rate (rate of myocardial deformation over time) can also be measured (Figure 4C and 4D).[27] Both methods improve functional assessment in akinetic segments tethered from normal myocardium that may have normal myocardial velocities. For the RV, strain imaging has been limited to the apical 4-chamber view (longitudinal strain). Circumferential shortening is assessed in short axis view and remains a research tool. RV myocardial velocities and deformation are impaired in PH patients, particularly at the apex.[37] Compared with spectral TDI, color TDI improves spatial resolution of RV wall motion. However, it still remains largely a research tool because of angle and frame rate dependence, complex post processing, low temporal resolution and relative lack of experience.

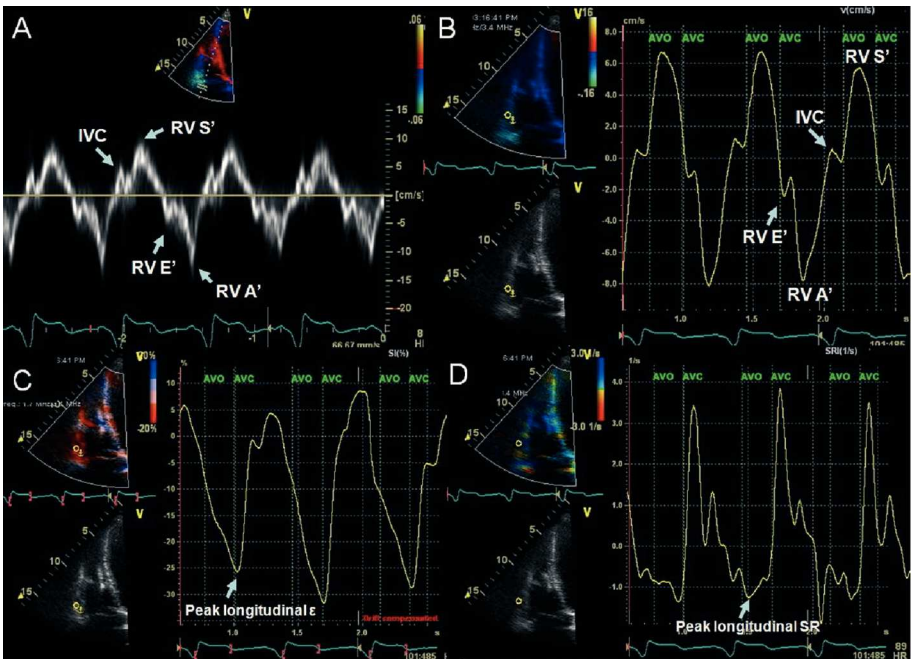

Figure 4. Example of tissue Doppler imaging (TDI) and strain imaging displayed in a subject with normal right ventricular (RV) function. A: spectral TDI waveforms of systolic and diastolic RV function from the lateral tricuspid annulus. B: color TDI phases with the sample volume placed at the basal RV wall. C: strain imaging with peak longitudinal systolic strain of –26 %, and D: strain rate of –1.4 s-1, both at the RV basal level. AVO indicates aortic valve opening; AVC, aortic valve closure; IVC, isovolumetric contraction peak positive velocity; RV A', atrial peak velocity (right atrial contraction); RV E', early diastolic peak velocity (during peak RV relaxation); RV S', systolic (ejection) peak velocity (during mechanical systole).

Similarly, evaluation of RV dyssynchrony with TDI is still in early stages of development.

Speckle Tracking

Speckle tracking analyzes motion by tracking speckles in the myocardium with an algorithm that identifies speckle location on sequential frames (velocity vector imaging) and derives strain values. It is less dependent on 2D image quality, frame rate, and angle, and has the ability to measure RV strain in both long and short axis planes. Several studies have shown that it is a feasible and accurate method to assess global and regional RV function in normal volunteers and PH patients.[38,39]

Intracardiac echocardiography

An intravascular ultrasound catheter can provide 2D, color and pulsed Doppler views of intracardiac structures. Preliminary data on animal models demonstrates the feasibility and accuracy of this technique for quantifying RV volumes, and systolic function.[40]

NUCLEAR IMAGING

Advantages of nuclear techniques include the lack of geometric assumptions for count-based methods of RV ejection fraction quantification, high contrast-to-noise ratio and the possibility of simultaneously evaluating pulmonary ventilation/perfusion (V/Q scan). Main drawbacks include limited spatial resolution, relatively prolonged imaging times and the need for radioisotopes. For the evaluation of the RV, many centers now prefer other modalities such as echocardiography or MRI that do not involve ionizing radiation and provide superior resolution.

First-pass radionuclide ventriculography is based on the detection and quantification with a gamma camera of the transit of a tracer bolus through the RV. The preferred agent is Technetium-99m labelled diethylenetriamine pentaacetate (^{99m}Tc-DTPA), which has a fast renal elimination, resulting in less patient irradiation and allowing earlier repetition of the study if necessary.[41] A quality bolus injection is crucial to provide enough RV counts, which will affect the accurate determination of RV ejection fraction. Normal values are 52% (6%) with a lower limit of 40%.[42] Although limited by imaging in a single plane, it allows good separation of the RV and right atrium, correlates well with right heart catheterization and MRI (although with large limits of agreement) and is considered the nuclear method of choice for RV assessment.[43,44]

Functional indices can also be obtained during a longer period and from multiple views with equilibrium blood pool scanning (Figure 5), which is technically less demanding. Planar imaging is limited because of overlap of the RV cavity with adjacent

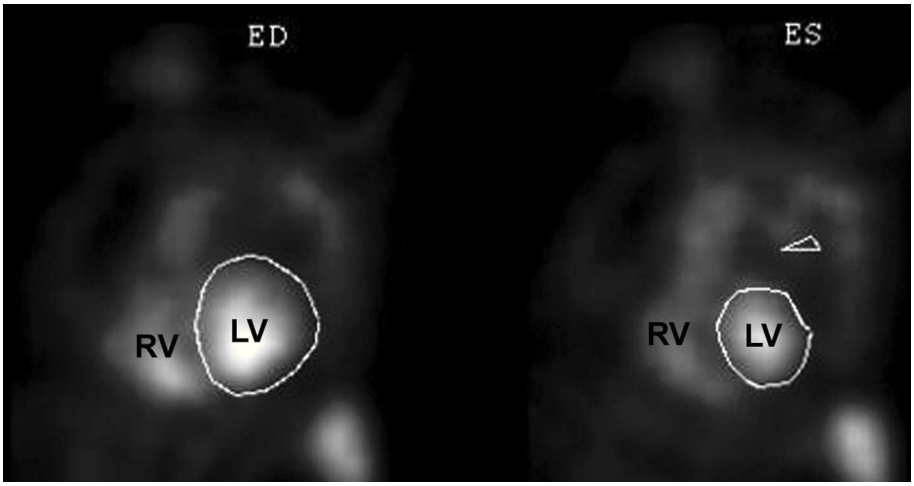

Figure 5. Left anterior oblique views of a gated blood pool scan after injection of red blood cell labeled in vivo with ^{99m}Tc-pertechnetate. ED indicates end-diastole; ES, end-systole; LV, left ventricle; RV, right ventricle. Courtesy of Dr. Milena Henzlova.

structures and is therefore not recommended.[44,45] A promising alternative is tomographic imaging, which is theoretically advantageous as it provides a true 3D dataset and allows for better separation of cardiac chambers. However, this technique has not been extensively validated.[43,46] Regarding myocardial imaging, preliminary data using positron emission tomography in patients with PH demonstrates increased uptake of ^{18}F-fluorodeoxyglucose in the RV free wall that correlates with disease severity and degree of RV overload.[47]

Lung V/Q scintigraphy is a well-validated modality for the evaluation of acute pulmonary embolism because embolic material will cause regional hypoperfusion with preserved ventilation. These areas of perfusion mismatch constitute the basis for diagnosis and also for grading the probability of embolism according to established criteria (Table 2 and Figure 6).[48] Although accurate, the relatively high rate of non-diagnostic intermediate probability scans represents one of the most important limitations of lung scintigraphy.[49] Tomographic imaging may improve image quality and diagnostic performance.[50] V/Q scanning is performed routinely in the diagnostic workup of patients with PH. Because CTEPH may be clinically indistinguishable from idiopathic PH, the possibility of chronic thromboembolism should be considered in the absence of known PH etiology. In general, a lung V/Q scan is considered the test of choice because of higher sensitivity than CT.[2,51] A normal or "low-probability" study portends a very low likelihood of CTEPH[52,53]; conversely, a relatively small perfusion defect on the V/Q scan may correspond to severe angiographic disease.[54]

INVASIVE ANGIOGRAPHY

Invasive angiography remains the gold standard for the evaluation of the pulmonary tree but has been largely replaced by noninvasive modalities. Both RV and pulmonary angiography are costly procedures and do not come without risk, with morbidity and mortality rates of 3.5%-6%, and 0.2%-0.5 %, respectively.[55] Complications may arise from arrhythmia, acute increase in pulmonary pressures related to acute volume overload or other mechanisms. They appear to be more common in patients with more severe PH and, particularly, more severe RV dysfunction.[56]

RV cineangiograms obtained after the administration of contrast through a pigtail or similar catheter (Figure 7) can provide accurate estimations of RV volumes and function applying Simpson's rule[57] or simplified analytical approaches.[58] These methods are nonetheless limited by the need for geometrical assumptions. Invasive pulmonary digital subtraction angiography (DSA) can be employed in the diagnosis of acute pulmonary embolism when results are inconclusive, although this is an infrequent indication.[49] However, DSA is commonly performed in the setting of chronic PH after a positive result in the lung V/Q scan. Typical angiographic signs of CTEPH include: abrupt branch tapering, complete vessel occlusion, luminal irregularities caused by mural clot, pouch-like regions related to occlusive or sub-occlusive thrombi, and webs or bands that may cause branch narrowing and post-stenotic dilatation (Figure 8).[59] It should be considered in patients with unexplained dyspnea and segmental or larger defects on ventilation-perfusion scanning,

TABLE 2. **Criteria for Thromboembolism by V/Q Scintigraphy**

High probability (>80%)	≥2 large mismatched segmental defects or the arithmetic equivalent
Intermediate probability (20%-79%)	1 moderate - 2 large mismatched segmental defects or the arithmetic equivalent
	1 matched defect with a clear chest x-ray
	Not described as low or high probability
Low probability (<19%)	Nonsegmental perfusion defects
	A defect smaller than the abnormality at chest x-ray
	Matched defects with normal chest x-ray and some areas of normal perfusion
	Small defects with a normal chest x-ray
Normal	No defects, perfusion outlines exactly the lungs on the chest x-ray

V/Q indicates ventilation/perfusion.
Large, moderate, and small defects are respectively defined as those involving >75%, 25%-75%, or <25% of a pulmonary segment. Adapted from Sostman HD et al.[48]

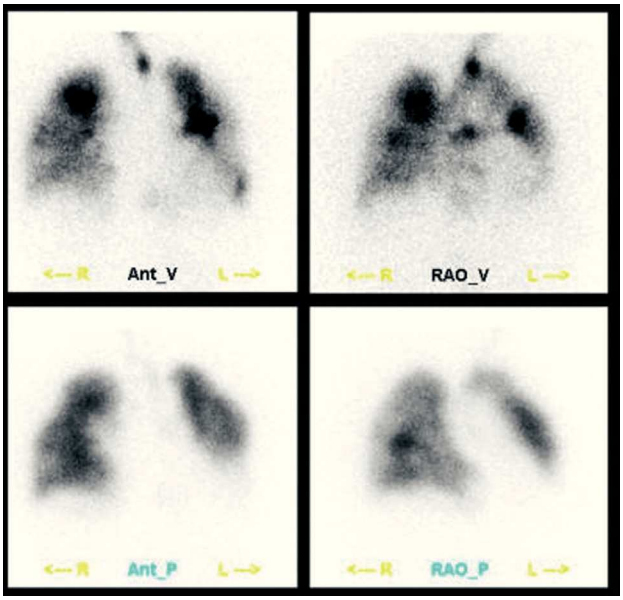

Figure 6. Ventilation (V; top row) and perfusion (P; bottom row) lung scintigraphy in a patient with thromboembolic disease, demonstrating areas of ventilation/perfusion mismatch in the lower lobes. Perfusion was studied with 99mTc-macroaggregated albumin and ventilation with Technetium-99m labelled diethylenetriamine pentaacetate (^{99m}Tc-DTPA). Ant indicates anterior; L, left; R, right; RAO, right anterior oblique. Courtesy of Dr. Josef Machac.

especially if there is echocardiographic evidence of right atrial enlargement or RV dysfunction. The purpose of DSA is to confirm the diagnosis of CTEPH and to define the location of occlusive emboli, as successful thromboendarterectomy is more likely if thrombi involve the main, lobar, or proximal segmental arteries.[60] DSA is still considered the procedure of choice for presurgical planning over alternative noninvasive modalities such as MRI and CT.[2,61] Inconclusive results of DSA may lead to further preoperative invasive imaging with fiberoptic angioscopy.[60]

COMPUTED TOMOGRAPHY

Contrast-enhanced CT angiography is the most commonly used technique for the evaluation of the pulmonary vasculature. It provides 3D datasets with excellent isotropic spatial resolution (sub-millimeter with current multidetector scanners) in very short scanning times. In addition, the lung parenchyma can be simultaneously evaluated and electrocardiographic gating allows for the study of cardiac function. On the other hand,

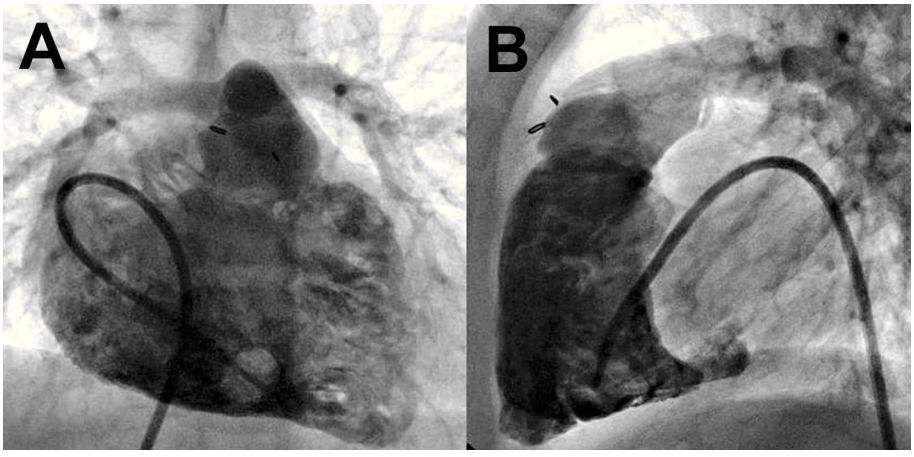

Figure 7. Biplane right heart contrast ventriculography in a child with repaired tetralogy of Fallot. A: anterior projection; B: lateral projection. Courtesy of Dr. Barry Love.

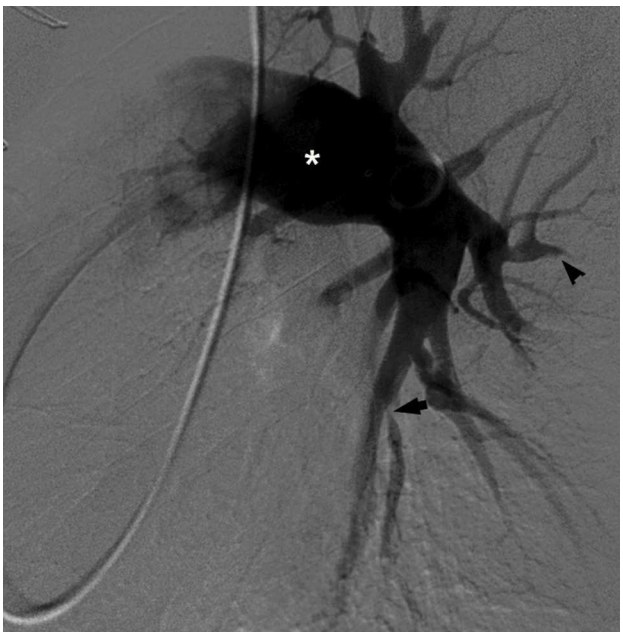

Figure 8. Digital subtraction angiography of the left pulmonary circulation in a patient with chronic thromboembolic pulmonary hypertension. There is dilatation of the central arteries (asterisk) as well as areas of luminal stenoses (arrow) and vessel occlusion (arrowhead). Courtesy of Dr. Robert Lookstein.

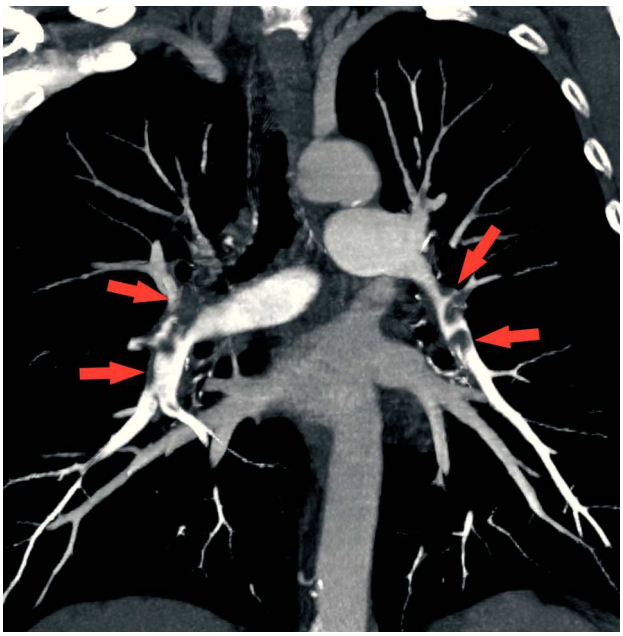

Figure 9. Coronal maximum intensity projection reconstruction of a computed tomography pulmonary angiogram in a patient with multiple, bilateral pulmonary embolisms (arrows).

CT offers only limited functional information (ie, flow) and requires iodinated contrast and ionizing radiation.

One of the most frequent indications is the suspicion of acute pulmonary embolism (Figure 9). Although DSA has been traditionally considered the gold standard, in clinical practice CT is the first test performed in most centers.[49] Reduced sensitivity for the detection of sub-segmental emboli has been considered the main limitation of CT, even though the probability of clinical recurrence in patients with a normal study is very low.[62] Multidetector scanners allow for the evaluation of pulmonary vessels down to 6th-order branches and appear to increase significantly the detection rate of distal pulmonary emboli. In the multicenter Prospective Investigation of Pulmonary Embolism Diagnosis II (PIOPED II) study, the sensitivity, specificity, positive predictive value and negative predictive value of multidetector CT angiography were 83%, 96%, 86%, and 95%, respectively.[63] In comparison with pulmonary V/Q scintigraphy, CT seems to diagnose a larger number of emboli.[64] In CTEPH, CT is also highly accurate and can depict a number of findings similar to those in DSA.[65] However, using invasive DSA as the gold standard, CTA is not yet considered sufficiently accurate to replace lung V/Q scintigraphy.[2]

CT can reveal other findings suggestive of PH, regardless of the underlying etiology. The degree of enlargement of central pulmonary arteries correlates moderately with disease severity and a ratio between the main PA and the ascending aorta diameters >1 or a main PA diameter ≥29 mm are fairly specific markers of PH, although with limited sensitivity.[66,67] An asymmetrical dilatation of the main arteries suggests CTEPH.[65] In patients with an acute pulmonary embolism, a right-left maximal ventricular diameter ratio >0.9 in a reformatted 4-chamber view independently predicts 30-day mortality.[68] Image acquisition with retrospective electrocardiographic gating has been validated as an accurate modality for the quantification of RV volumes and function in comparison with magnetic resonance (Figure 10), although at the expense of increased radiation dose.[69] The feasibility of detecting RV dysfunction in patients with an acute pulmonary embolism has been reported[70]; however, its prognostic significance or its application in chronic PH have not been tested systematically.

Simultaneous evaluation of the lung parenchyma may point to specific etiologies of PH, as many features of obstructive or interstitial lung disease can be readily identified. A mosaic pattern in combination with signs of PH may be caused

by heterogeneous lung perfusion and is highly suggestive of CTEPH.[71] Prior pulmonary infarcts (wedge-shaped consolidations in subpleural regions) also support the diagnosis of CTEPH.[65] Other indirect signs of increased systemic venous pressure include enlargement of the superior and inferior vena cava, ascitis and pericardial and/or pleural effusions.

MAGNETIC RESONANCE IMAGING

MRI has evolved in the last decade as one of the most attractive imaging modalities for the study of both the right heart and the pulmonary circulation.[72,73] It has a good balance of high spatial, temporal and contrast resolution, can obtain images in any desired orientation and has no "acoustic" window limitations. It is also safe, highly accurate and reproducible, and provides both anatomic and functional information. The main limitations are cost, less widespread availability and experience, and constraints related to the magnetic field. In addition, there has been concern on the potential association of gadolinium contrast agents with nephrogenic systemic fibrosis. In the specific context of PH, MRI has limited ability to quantify PA pressures.[74]

Evaluation of the RV

MRI is currently considered the gold standard for the quantification of RV volumes and ejection fraction.[31] The most commonly employed approach is to apply Simpson's method to a stack of contiguous short-axis cine loops acquired from base to apex. This approach is highly accurate and does not rely on geometrical assumptions.[73,75] The good interstudy reproducibility also indicates a role for MRI in the serial follow-up of patients, for example in the evaluation of the effect of therapies.[76] The degree of RV dilatation, hypertrophy and systolic dysfunction is directly proportional to the severity of PH. As an example, an RV to left ventricular mass ratio >0.6 detects PH with a sensitivity of 84% and a specificity of 71% and has been reported to be more specific than Doppler echocardiography.[77] Importantly, quantification of RV functional parameters appears to add prognostic information, as demonstrated in a study of patients with idiopathic PH in whom a RV end-diastolic volume index ≥84 mL/m^2 and a left ventricular end-diastolic volume index ≤40 mL/m^2 were independent predictors of 1-year mortality.[78] More sophisticated analyses of RV performance can be obtained with simultaneous quantification of pressures with MRI-compatible catheters to derive RV volume/pressure loops.[79] Myocardial tagging has been used to detect abnormal regional RV strain patterns in PH, although this technique has limited resolution and requires long post-processing times. These limitations can be overcome with recently developed strain encoded MRI.[80] Alternatively, myocardial velocities can be quantified using phase-contrast imaging in a manner similar to DTI.[81]

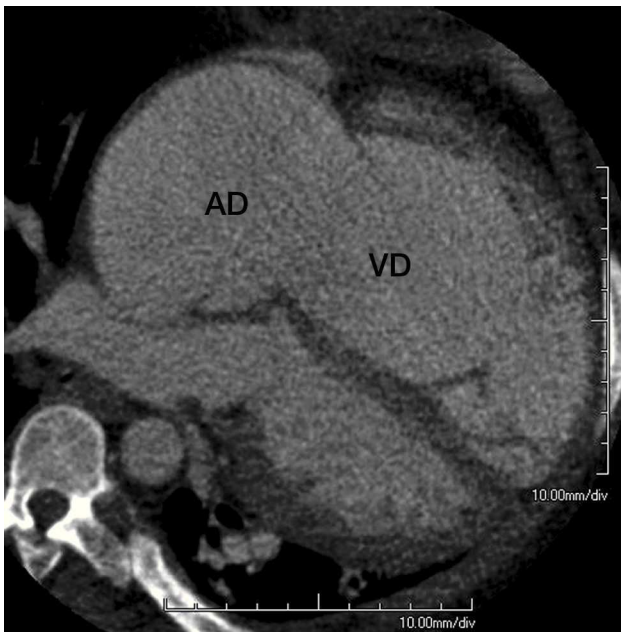

Figure 10. Multiplanar reformation in a 4-chamber view orientation of cardiac computed tomography in a patient with severe right atrial (RA) and right ventricular (RV) enlargement due to tricuspid regurgitation.

MRI can also be employed to quantify interventricular septal curvature (Figure 11), defined as the inverse of the radius. End-systolic septal curvature correlates strongly with PH severity and leftwards septal bowing has been associated with a systolic PA pressure >67 mm Hg.[82] The comparison between the curvatures of the interventricular septum and of the left ventricular free wall can also be used to quantify systolic PA pressure accurately.[83] Delayed contrast enhancement indicative of fibrosis can be noted in PH patients at the level of the septal insertion sites of the RV and often extending into the interventricular septum, a finding associated with paradoxical septal motion. The extent of fibrosis correlates directly with the degree of PH and is seen irrespective of PH etiology, probably representing increased mechanical stress at these points.[84,85] It is currently unknown if this finding carries clinical implications.

Evaluation of the Pulmonary Circulation

High-resolution magnetic resonance angiography can be employed to detect pulmonary emboli or

depict typical features of chronic PH or CTEPH.[86,87] Using this approach, preliminary reports suggest good diagnostic accuracy for the differentiation of idiopathic PH from CTEPH.[87] In comparison with DSA and CT, MRI offers excellent depiction of proximal abnormalities but accuracy is lower for subsegmental vessels.[49,86,87] In addition, time-resolved magnetic resonance angiography can be used to visualize the dynamic passage of the contrast through the lung vasculature (Figure 12). This technique can be employed to analyze lung perfusion in a manner that correlates well with nuclear scintigraphy.[87,88] Preliminary data also demonstrates the feasibility of evaluating lung ventilation with MRI.[89]

Measurement of blood velocities with phase-contrast imaging is usually employed for the accurate quantification of systemic-to-pulmonary flow ratios in patients with congenital shunts.[90] In addition, flow profiles in the cross-section of the main PA or its branches can be accurately characterized.[91] Numerous parameters have shown correlation with the degree of elevation of PA pressures and/or resistance, although with inconsistent results.[74] An average blood flow velocity <11.7 cm/s provides a sensitivity and specificity of 93% and 82%, respectively, for the detection of PH.[92] More recently, 3D phase-contrast MRI revealed abnormal patterns in the main PA (end-systolic flow vortices and prolonged anterograde diastolic flows) that enabled differentiating patients with PH at rest, exercise-induced PH or no PH.[93] In addition, phase-contrast or cine imaging can be employed to evaluate dynamic changes in arterial cross-section and therefore pulmonary artery stiffness.[94] A change in PA cross-sectional area <16% during the cardiac cycle was identified recently as a predictor of mortality in PH.[95] Also, alterations in PA elasticity can be detected before overt PH occurs and these may be useful for early detection of abnormal circulatory physiology.[96]

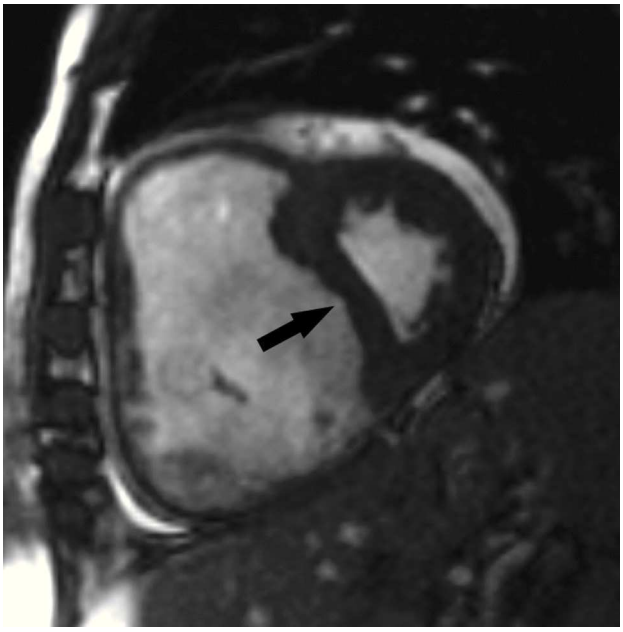

Figure 11. PShort axis view obtained with magnetic resonance imaging in a patient with severe pulmonary hypertension. There is severe enlargement of the right ventricle which leads to septal bowing (arrow) and compression of the left ventricle.

CONCLUSION

Several imaging modalities can be combined today for the evaluation of the right heart and the pulmonary circulation. Advances in nuclear techniques, echocardiography, CT and MRI have expanded our understanding of the crucial roles of the minor circulatory system in many pathologic states. Continuing technological advances, particularly in the field of MRI, promise to further improve our ability to detect early disease stages or evaluate the mechanisms of action and efficacy of novel therapeutic interventions Advances in molecular imaging with any of these modalities will be of particular interest in the evaluation of multiple biological processes in vivo.

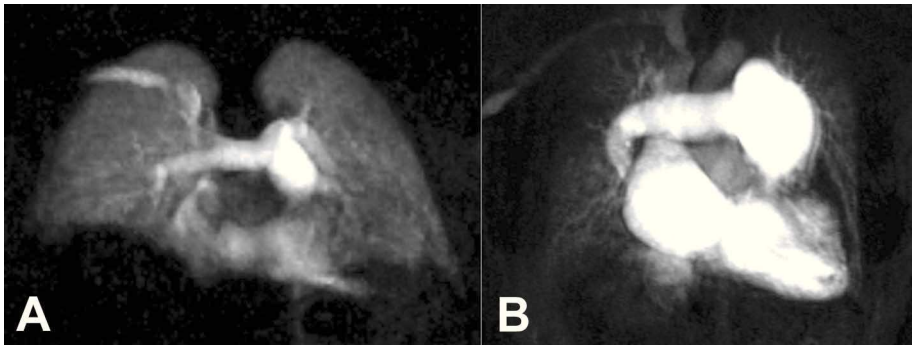

Figure 12. Coronal time-resolved magnetic resonance angiography in a normal subject (A) and in a patient with idiopathic pulmonary hypertension (B). Note the central pulmonary artery enlargement and the diffuse peripheral hypoperfusion in the patient with pulmonary hypertension.

REFERENCES

1. Boxt LM. Radiology of the right ventricle. Radiol Clin North Am. 1999;37:379-400.
2. McGoon M, Gutterman D, Steen V, Barst R, McCrory DC, Fortin TA, et al. Screening, early detection, and diagnosis of pulmonary arterial hypertension: ACCP evidence-based clinical practice guidelines. Chest. 2004;126:14S-34S.
3. Lupi E, Dumont C, Tejada VM, Horwitz S, Galland F. A radiologic index of pulmonary arterial hypertension. Chest. 1975;68:28-31.
4. Matthay RA, Schwarz MI, Ellis JH, Steele PP, Siebert PE, Durrance JR, et al. Pulmonary artery hypertension in chronic obstructive pulmonary disease: determination by chest radiography. Invest Radiol. 1981;16:95-100.
5. Galié N, Torbicki A, Barst R, Dartevelle P, Haworth S, Higenbottam T, et al. Guías de Práctica Clínica sobre el diagnóstico y tratamiento de la hipertensión arterial pulmonar. Rev Esp Cardiol. 2005;58:523-66.
6. Lang RM, Bierig M, Devereux RB, Flachskampf FA, Foster E, Pellikka PA, et al. Recommendations for chamber quantification: a report from the American Society of Echocardiography's Guidelines and Standards Committee and the Chamber Quantification Writing Group, developed in conjunction with the European Association of Echocardiography, a branch of the European Society of Cardiology. J Am Soc Echocardiogr. 2005;18:1440-63.
7. Matsukubo H, Matsuura T, Endo N, Asayama J, Watanabe T. Echocardiographic measurement of right ventricular wall thickness. A new application of subxiphoid echocardiography. Circulation. 1977;56:278-84.
8. Louie EK, Rich S, Levitsky S, Brundage BH. Doppler echocardiographic demonstration of the differential effects of right ventricular pressure and volume overload on left ventricular geometry and filling. J Am Coll Cardiol. 1992;19:84-90.
9. Raymond RJ, Hinderliter AL, Willis PWIV, Ralph D, Caldwell EJ, Williams W, et al. Echocardiographic predictors of adverse outcomes in primary pulmonary hypertension. J Am Coll Cardiol. 2002;39:1214-9.
10. King ME, Braun H, Goldblatt A, Liberthson R, Weyman AE. Interventricular septal configuration as a predictor of right ventricular systolic hypertension in children: a cross-sectional echocardiographic study. Circulation. 1983;68:68-75.
11. Forfia PR, Fisher MR, Mathai SC, Housten-Harris T, Hemnes AR, Borlaug BA, et al. Tricuspid annular displacement predicts survival in pulmonary hypertension. Am J Respir Crit Care Med. 2006;174:1034-41.
12. Ueti OM, Camargo EE, Ueti Ade A, de Lima-Filho EC, Nogueira EA. Assessment of right ventricular function with Doppler echocardiographic indices derived from tricuspid annular motion: comparison with radionuclide angiography. Heart. 2002;88:244-8.
13. Anavekar NS, Gerson D, Skali H, Kwong RY, Yucel EK, Solomon SD. Two-dimensional assessment of right ventricular function: an echocardiographic-MRI correlative study. Echocardiography. 2007;24:452-6.
14. Tei C, Dujardin KS, Hodge DO, Bailey KR, McGoon MD, Tajik AJ, et al. Doppler echocardiographic index for assessment of global right ventricular function. J Am Soc Echocardiogr. 1996;9:838-47.
15. Yeo TC, Dujardin KS, Tei C, Mahoney DW, McGoon MD, Seward JB. Value of a Doppler-derived index combining systolic and diastolic time intervals in predicting outcome in primary pulmonary hypertension. Am J Cardiol. 1998;81:1157-61.
16. Karnati PK, El-Hajjar M, Torosoff M, Fein SA. Myocardial performance index correlates with right ventricular ejection fraction measured by nuclear ventriculography. Echocardiography. 2008;25:381-5.
17. Eysmann SB, Palevsky HI, Reichek N, Hackney K, Douglas PS. Two-dimensional and Doppler-echocardiographic and cardiac catheterization correlates of survival in primary pulmonary hypertension. Circulation. 1989;80:353-60.
18. Vlahos AP, Feinstein JA, Schiller NB, Silverman NH. Extension of Doppler-derived echocardiographic measures of pulmonary vascular resistance to patients with moderate or severe pulmonary vascular disease. J Am Soc Echocardiogr. 2008;21:711-4.
19. Abbas AE, Fortuin FD, Schiller NB, Appleton CP, Moreno CA, Lester SJ. A simple method for noninvasive estimation of pulmonary vascular resistance. J Am Coll Cardiol. 2003;41:1021-7.
20. Tolle JJ, Waxman AB, van Horn TL, Pappagianopoulos PP, Systrom DM. Exercise-induced pulmonary arterial hypertension. Circulation. 2008;118:2183-9.
21. Solis J, Sitges M, Levine RA, Hung J. Ecocardiografía tridimensional. Nuevas perspectivas sobre la caracterización de la válvula mitral. Rev Esp Cardiol. 2009;62:188-98.
22. Jiang L, Siu SC, Handschumacher MD, Luis Guererro J, Vázquez de Prada JA, King ME, et al. Three-dimensional echocardiography. In vivo validation for right ventricular volume and function. Circulation. 1994;89:2342-50.
23. Shiota T, Jones M, Chikada M, Fleishman CE, Castellucci JB, Cotter B, et al. Real-time three-dimensional echocardiography for determining right ventricular stroke volume in an animal model of chronic right ventricular volume overload. Circulation. 1998;97:1897-900.
24. Lu X, Nadvoretskiy V, Bu L, Stolpen A, Ayres N, Pignatelli RH, et al. Accuracy and reproducibility of real-time three-dimensional echocardiography for assessment of right ventricular volumes and ejection fraction in children. J Am Soc Echocardiogr. 2008;21:84-9.
25. Liang XC, Cheung EW, Wong SJ, Cheung YF. Impact of right ventricular volume overload on three-dimensional global left ventricular mechanical dyssynchrony after surgical repair of tetralogy of Fallot. Am J Cardiol. 2008;102:1731-6.
26. Ton-Nu TT, Levine RA, Handschumacher MD, Dorer DJ, Yosefy C, Fan D, et al. Geometric determinants of functional tricuspid regurgitation: insights from 3-dimensional echocardiography. Circulation. 2006;114:143-9.
27. Gallego García de Vinuesa P, Velasco del Castillo S, Aguilar Torres R, Pare Bardera JC. Actualización en técnicas de imagen cardiaca. Ecocardiografía, resonancia magnética y tomografía computarizada. Rev Esp Cardiol. 2008;61:109-31.
28. Sukmawan R AT, Watanabe N, Akiyama M, Wada N, Taniguchi M, Kawamoto T,Yoshida K. Quantitative assessment of right ventricular geometric remodeling in pulmonary hypertension secondary to left-sided heart disease using real-time three-dimensional echocardiography. Am J Cardiol. 2004;94:1096-9.
29. Meluzin J, Spinarova L, Bakala J, Toman J, Krejci J, Hude P, et al. Pulsed Doppler tissue imaging of the velocity of tricuspid annular systolic motion; a new, rapid, and non-invasive method of evaluating right ventricular systolic function. Eur Heart J. 2001;22:340-8.

30. Lindqvist P, Waldenstrom A, Henein M, Morner S, Kazzam E. Regional and global right ventricular function in healthy individuals aged 20-90 years: a pulsed Doppler tissue imaging study: Umea General Population Heart Study. Echocardiography. 2005;22:305-14.
31. Champion HC ME, Hassoun PM. Comprehensive invasive and noninvasive approach to the right ventricle-pulmonary circulation unit: state of the art and clinical and research implications. Circulation. 2009;120:992-1007.
32. Ruan Q, Nagueh SF. Clinical Application of Tissue Doppler Imaging in Patients With Idiopathic Pulmonary Hypertension. Chest. 2007;131:395-401.
33. Duan YY, Harada K, Toyono M, Ishii H, Tamura M, Takada G. Effects of acute preload reduction on myocardial velocity during isovolumic contraction and myocardial acceleration in pediatric patients. Pediatr Cardiol. 2006;27:32-6.
34. Caso P, Galderisi M, Cicala S, Cioppa C, D'Andrea A, Lagioia G, et al. Association between myocardial right ventricular relaxation time and pulmonary arterial pressure in chronic obstructive lung disease: analysis by pulsed Doppler tissue imaging. J Am Soc Echocardiogr. 2001;14:970-7.
35. Fahmy Elnoamany M, Abdelraouf Dawood A. Right ventricular myocardial isovolumic relaxation time as novel method for evaluation of pulmonary hypertension: correlation with endothelin-1 levels. J Am Soc Echocardiogr. 2007;20: 462-9.
36. Kukulski T, Hubbert L, Arnold M, Wranne B, Hatle L, Sutherland GR. Normal regional right ventricular function and its change with age: a Doppler myocardial imaging study. J Am Soc Echocardiogr. 2000;13:194-204.
37. Huez S, Vachiery JL, Unger P, Brimioulle S, Naeije R. Tissue Doppler imaging evaluation of cardiac adaptation to severe pulmonary hypertension. Am J Cardiol. 2007;100:1473-8.
38. Vitarelli A, Conde Y, Cimino E, Stellato S, D'Orazio S, D'Angeli I, et al. Assessment of right ventricular function by strain rate imaging in chronic obstructive pulmonary disease. Eur Respir J. 2006;27:268-75.
39. Teske AJ, de Boeck BW, Olimulder M, Prakken NH, Doevendans PA, Cramer MJ. Echocardiographic assessment of regional right ventricular function: a head-to-head comparison between 2-dimensional and tissue Doppler-derived strain analysis. J Am Soc Echocardiogr. 2008;21:275-83.
40. Vázquez de Prada JA, Chen MH, Guerrero JL, Padial LR, Jiang L, Schwammenthal E, et al. Ventricular Function Intracardiac echocardiography: In vitro and in vivo validation for right ventricular volume and function. Am Heart J. 1996;131:320-8.
41. Candell Riera J, Castell Conesa J, Jurado López JA, López de Sá E, Nuño de la Rosa JA, Ortigosa Aso FJ. Et al. Guías de actuación clínica de la Sociedad Española de Cardiología. Cardiología nuclear: bases técnicas y aplicaciones clínicas. Rev Esp Cardiol. 1999;52:957-89.
42. Pfisterer ME, Battler A, Zaret BL. Range of normal values for left and right ventricular ejection fraction at rest and during exercise assessed by radionuclide angiocardiography. Eur Heart J. 1985;6:647-55.
43. Andreas K, Anne-Mette L, Birger H, Claus Leth P. Right-sided cardiac function in healthy volunteers measured by first-pass radionuclide ventriculography and gated blood-pool SPECT: comparison with cine MRI. Clin Physio Funct Imag. 2005;25:344-9.
44. Hesse B, Lindhardt TB, Acampa W, Anagnostopoulos C, Ballinger J, Bax JJ, et al. EANM/ESC guidelines for radionuclide imaging of cardiac function. Eur J Nucl Med Mol Imaging. 2008;35:851-85.
45. Corbett JR, Akinboboye OO, Bacharach SL, Borer JS, Botvinick EH, DePuey EG, et al. Equilibrium radionuclide angiocardiography. J Nucl Cardiol. 2006;13:e56-79.
46. Hacker M, Hoyer X, Kupzyk S, La Fougere C, Kois J, Stempfle HU, et al. Clinical validation of the gated blood pool SPECT QBS processing software in congestive heart failure patients: correlation with MUGA, first-pass RNV and 2D-echocardiography. Int J Cardiovasc Imaging. 2006;22: 407-16.
47. Oikawa M, Kagaya Y, Otani H, Sakuma M, Demachi J, Suzuki J, et al. Increased [18F]Fluorodeoxyglucose Accumulation in Right Ventricular Free Wall in Patients With Pulmonary Hypertension and the Effect of Epoprostenol. J Am Coll Cardiol. 2005;45:1849-55.
48. Sostman HD, Coleman RE, DeLong DM, Newman GE, Paine S. Evaluation of revised criteria for ventilation-perfusion scintigraphy in patients with suspected pulmonary embolism. Radiology. 1994;193:103-7.
49. Torbicki A, Perrier A, Konstantinides S, Agnelli G, Galiè N, et al. Guidelines on the diagnosis and management of acute pulmonary embolism: The Task Force for the Diagnosis and Management of Acute Pulmonary Embolism of the European Society of Cardiology (ESC). Eur Heart J. 2008;29:2276-315.
50. Roach PJ, Bailey DL, Harris BE. Enhancing lung scintigraphy with single-photon emission computed tomography. Semin Nucl Med. 2008;38:441-9.
51. Tunariu N, Gibbs SJ, Win Z, Gin-Sing W, Graham A, Gishen P, et al. Ventilation-perfusion scintigraphy is more sensitive than multidetector CTPA in detecting chronic thromboembolic pulmonary disease as a treatable cause of pulmonary hypertension. J Nucl Med. 2007;48:680-4.
52. D'Alonzo GE, Bower JS, Dantzker DR. Differentiation of patients with primary and thromboembolic pulmonary hypertension. Chest. 1984;85:457-61.
53. Worsley DF, Palevsky HI, Alavi A. Ventilation-perfusion lung scanning in the evaluation of pulmonary hypertension. J Nucl Med. 1994;35:793-6.
54. Ryan KL, Fedullo PF, Davis GB, Vasquez TE, Moser KM. Perfusion scan findings understate the severity of angiographic and hemodynamic compromise in chronic thromboembolic pulmonary hypertension. Chest. 1988;93:1180-5.
55. Schoepf UJ, Goldhaber SZ, Costello P. Spiral computed tomography for acute pulmonary embolism. Circulation. 2004;109:2160-7.
56. Perlmutt LM, Braun SD, Newman GE, Oke EJ, Dunnick NR. Pulmonary arteriography in the high-risk patient. Radiology. 1987;162:187-9.
57. Gentzler RD, Briselli MF, Gault JH. Angiographic estimation of right ventricular volume in man. Circulation. 1974;50:324-30.
58. Ferlinz J, Gorlin R, Cohn PF, Herman MV. Right ventricular performance in patients with coronary artery disease. Circulation. 1975;52:608-15.
59. Auger WR, Fedullo PF, Moser KM, Buchbinder M, Peterson KL. Chronic major-vessel thromboembolic pulmonary artery obstruction: appearance at angiography. Radiology. 1992;182:393-8.
60. Fedullo PF, Auger WR, Kerr KM, Rubin LJ. Chronic Thromboembolic Pulmonary Hypertension. N Engl J Med. 2001;345:1465-72.

61. Lang IM, Klepetko W. Actualización sobre la hipertensión pulmonar tromboembólica crónica, una enfermedad que a menudo no se detecta. Rev Esp Cardiol. 2009;62:120-5.
62. Quiroz R, Kucher N, Zou KH, Kipfmueller F, Costello P, Goldhaber SZ, et al. Clinical validity of a negative computed tomography scan in patients with suspected pulmonary embolism: a systematic review. JAMA. 2005;293:2012-7.
63. Stein PD, Fowler SE, Goodman LR, Gottschalk A, Hales CA, Hull RD, et al. Multidetector Computed Tomography for Acute Pulmonary Embolism. N Engl J Med. 2006;354:2317-27.
64. Anderson DR, Kahn SR, Rodger MA, Kovacs MJ, Morris T, Hirsch A, et al. Computed Tomographic Pulmonary Angiography vs Ventilation-Perfusion Lung Scanning in Patients With Suspected Pulmonary Embolism: A Randomized Controlled Trial. JAMA. 2007;298:2743-53.
65. King MA, Ysrael M, Bergin CJ. Chronic thromboembolic pulmonary hypertension: CT findings. AJR Am J Roentgenol. 1998;170:955-60.
66. Kuriyama K, Gamsu G, Stern RG, Cann CE, Herfkens RJ, Brundage BH. CT-determined pulmonary artery diameters in predicting pulmonary hypertension. Invest Radiol. 1984;19:16-22.
67. Ng CS, Wells AU, Padley SP. A CT sign of chronic pulmonary arterial hypertension: the ratio of main pulmonary artery to aortic diameter. J Thorac Imaging. 1999;14:270-8.
68. Schoepf UJ, Kucher N, Kipfmueller F, Quiroz R, Costello P, Goldhaber SZ. Right ventricular enlargement on chest computed tomography: a predictor of early death in acute pulmonary embolism. Circulation. 2004;110:3276-80.
69. Plumhans C, Muhlenbruch G, Rapaee A, Sim KH, Seyfarth T, Gunther RW, et al. Assessment of global right ventricular function on 64-MDCT compared with MRI. AJR Am J Roentgenol. 2008;190:1358-61.
70. Dogan H, Kroft LJ, Huisman MV, van der Geest RJ, de Roos A. Right ventricular function in patients with acute pulmonary embolism: analysis with electrocardiography-synchronized multi-detector row CT. Radiology. 2007;242:78-84.
71. Sherrick AD, Swensen SJ, Hartman TE. Mosaic pattern of lung attenuation on CT scans: frequency among patients with pulmonary artery hypertension of different causes. AJR Am J Roentgenol. 1997;169:79-82.
72. Fuster V, Sanz J. Hipertensión pulmonar: nuevos conocimientos a través de tecnología de imagen. Rev Esp Cardiol. 2007;60 Supl 3:2-9.
73. Pamboucas C, Nihoyannopoulos P. Papel de la resonancia magnética cardiovascular en el diagnóstico y evaluación de la hipertensión arterial pulmonar. Rev Esp Cardiol. 2006;59: 755-60.
74. Roeleveld RJ, Marcus JT, Boonstra A, Postmus PE, Marques KM, Bronzwaer JGF, et al. A comparison of noninvasive MRI-based methods of estimating pulmonary artery pressure in pulmonary hypertension. J Magn Reson Imaging. 2005;22: 67-72.
75. Shors SM, Fung CW, Francois CJ, Finn JP, Fieno DS. Accurate Quantification of Right Ventricular Mass at MR Imaging by Using Cine True Fast Imaging with Steady-State Precession: Study in Dogs. Radiology. 2004;230:383-8.
76. Grothues F, Moon JC, Bellenger NG, Smith GS, Klein HU, Pennell DJ. Interstudy reproducibility of right ventricular volumes, function, and mass with cardiovascular magnetic resonance. Am Heart J .2004;147:218-23.
77. Saba TS, Foster J, Cockburn M, Cowan M, Peacock AJ. Ventricular mass index using magnetic resonance imaging accurately estimates pulmonary artery pressure. Eur Respir J. 2002;20:1519-24.
78. van Wolferen SA, Marcus JT, Boonstra A, Marques KM, Bronzwaer JG, Spreeuwenberg MD, et al. Prognostic value of right ventricular mass, volume, and function in idiopathic pulmonary arterial hypertension. Eur Heart J. 2007;28:1250-7.
79. Kuehne T, Yilmaz S, Steendijk P, Moore P, Groenink M, Saaed M, et al. Magnetic resonance imaging analysis of right ventricular pressure-volume loops: in vivo validation and clinical application in patients with pulmonary hypertension. Circulation. 2004;110:2010-6.
80. Youssef A, Ibrahim el-SH, Korosoglou G, Abraham MR, Weiss RG, Osman NF. Strain-encoding cardiovascular magnetic resonance for assessment of right ventricular regional function. J Cardiovasc Magn Reson. 208;10:1-10.
81. Kayser HW, van der Geest RJ, van der Wall EE, Duchateau C, de Roos A. Right ventricular function in patients after acute myocardial infarction assessed with phase contrast MR velocity mapping encoded in three directions. J Magn Reson Imaging. 2000;11:471-5.
82. Roeleveld RJ, Marcus JT, Faes TJ, Gan TJ, Boonstra A, Postmus PE, et al. Interventricular septal configuration at MR imaging and pulmonary arterial pressure in pulmonary hypertension. Radiology. 2005;234:710-7.
83. Dellegrottaglie S, Sanz J, Poon M, Viles-González JF, Sulica R, Goyenechea M, et al. Pulmonary hypertension: accuracy of detection with left ventricular septal-to-free wall curvature ratio measured at cardiac MR. Radiology. 2007;243:63-9.
84. Blyth KG, Groenning BA, Martin TN, Foster JE, Mark PB, Dargie HJ, et al. Contrast enhanced-cardiovascular magnetic resonance imaging in patients with pulmonary hypertension. Eur Heart J. 2005;26:1993-9.
85. Sanz J, Dellegrottaglie S, Kariisa M, Sulica R, Poon M, O'Donnell TP, et al. Prevalence and correlates of septal delayed contrast enhancement in patients with pulmonary hypertension. Am J Cardiol. 2007;100:731-5.
86. Kreitner KF, Ley S, Kauczor HU, Mayer E, Kramm T, Pitton MB, et al. Chronic thromboembolic pulmonary hypertension: pre- and postoperative assessment with breath-hold MR imaging techniques. Radiology. 2004;232:535-43.
87. Nikolaou K, Schoenberg SO, Attenberger U, Scheidler J, Dietrich O, Kuehn B, et al. Pulmonary Arterial Hypertension: Diagnosis with Fast Perfusion MR Imaging and High-Spatial-Resolution MR Angiography--Preliminary Experience. Radiology. 2005;236:694-703.
88. Ohno Y, Hatabu H, Murase K, Higashino T, Kawamitsu H, Watanabe H, et al. Quantitative assessment of regional pulmonary perfusion in the entire lung using three-dimensional ultrafast dynamic contrast-enhanced magnetic resonance imaging: Preliminary experience in 40 subjects. J Magn Reson Imaging. 2004;20:353-65.
89. Ohno Y, Hatabu H, Takenaka D, Adachi S, van Cauteren M, Sugimura K. Oxygen-Enhanced MR Ventilation Imaging of the Lung: Preliminary Clinical Experience in 25 Subjects. AJR Am J Roentgenol. 2001;177:185-94.
90. Hundley WG, Li HF, Lange RA, Pfeifer DP, Meshack BM, Willard JE, et al. Assessment of Left-to-Right Intracardiac Shunting by Velocity-Encoded, Phase-Difference Magnetic Resonance Imaging: A Comparison With Oximetric and Indicator Dilution Techniques. Circulation. 1995;91:2955-60.

91. Kondo C, Caputo GR, Masui T, Foster E, O'Sullivan M, Stulbarg MS, et al. Pulmonary hypertension: pulmonary flow quantification and flow profile analysis with velocity-encoded cine MR imaging. Radiology. 1992;183:751-8.

92. Sanz J, Kuschnir P, Rius T, Salguero R, Sulica R, Einstein AJ, et al. Pulmonary arterial hypertension: noninvasive detection with phase-contrast MR imaging. Radiology. 2007;243:70-9.

93. Reiter G, Reiter U, Kovacs G, Kainz B, Schmidt K, Maier R, et al. Magnetic resonance-derived 3-dimensional blood flow patterns in the main pulmonary artery as a marker of pulmonary hypertension and a measure of elevated mean pulmonary arterial pressure. Circ Cardiovasc Imaging. 2008;1:23-30.

94. Paz R, Mohiaddin RH, Longmore DB. Magnetic resonance assessment of the pulmonary arterial trunk anatomy, flow, pulsatility and distensibility. Eur Heart J. 1993;14:1524-30.

95. Gan CT-J, Lankhaar J-W, Westerhof N, Marcus JT, Becker A, Twisk JWR, et al. Noninvasively Assessed Pulmonary Artery Stiffness Predicts Mortality in Pulmonary Arterial Hypertension. Chest. 2007;132:1906-12.

96. Sanz J, Kariisa M, Dellegrottaglie S, Prat-González S, García MJ, Fuster V, et al. Evaluation of pulmonary artery stiffness in pulmonary hypertension with cardiac magnetic resonance. JACC Cardiovasc Imaging. 2009;2:286-95.